

# SEA SURFACE CURRENT RETRIEVING FROM TANDEM-X DATA SATELLITE DATA

Maged Marghany  
Geoinformation Global Space Technology  
130B, Jalan Burhanuddin Helmi,  
Taman Tun Dr. Ismail,  
60000 Kuala Lumpur  
Email:magedupm@hotmail.com

**KEYWORDS** : TANDEM-X satellite, Multi-objective evolutionary algorithm, Hopfield neural network, ocean current, Pareto front.

**ABSTRACT:** This is first work is done on application of TanDEM-X data satellite data to Malaysian coastal waters. This aims at utilizing an optimization of Hopfield neural network to retrieve variation of sea surface current along Malaysian coastal waters. In doing so, multi-objective evolutionary algorithm based on Pareto front is used to minimize the error has produced due to non-linearity between TanDEM-X data and sea surface movements. This work aimed at retrieving sea surface current from TanDEM-X data along the coastal water of Malaysia. Two approaches have been implemented Hopfield neural network algorithm and Pareto optimal solution. The study shows that the Pareto optimal solution has highest performance than Hopfield neural network algorithm with lowest RMSE of  $\pm 0.009$ . Further, Pareto optimal solution can determine the sea surface current pattern variation along coastal water from TanDEM-X data. In conclusion, TanDEM-X data shows an excellent promises for retrieving sea surface.

## 1. INTRODUCTION

Synthetic aperture radar (SAR) is recognized because the potential tool for dynamic earth science studies. One of an attention-grabbing topic is current flow that is needed short go back satellite cycle and high resolution. These will give exactly data concerning current dynamic flow (Marghany 2000 and Krieger et al., 2003). In fact, current is very important for ship navigation, fishing, waste matter substances transport and sediment transport. Respectively optical and microwave sensors are enforced to monitor the current flows. Indeed, the ocean surface dynamic options of sea surface current is vital parameters for atmospheric-sea surface interactions. In this regard, the global climate change, marine pollution and coastal risky are preponderantly dominated by current speed and direction (Alejandro and Saadon 1996; Alejandro and Demmler 1997; Inglada and Garello 2002). The measurements of ocean current from space relies on the electromagnetic signal. Truly, associate degree of an electromagnetic signal of optical and microwave reflects from the ocean carrying records concerning one among the first discernible quantities that are the colour, the beamy temperature, the roughness, and also the height of the ocean (Inglada and Garello 2002 and Romeiser et al., 2010).

The principal conception to retrieve the ocean surface current from SAR information is perform of the Doppler frequency shift theory (Marghany 2009a). Incidentally, the orbital quality of the ocean wave and surface current dynamic interactions will cause shifting of the radiolocation signal within the angle direction i.e. the flight direction that is thought because the Doppler frequency shift (Cao and Wang 2003). In truth, the surface current dynamic is virtual to the orbital movement and an antenna rotation of the synthetic aperture radar. Consequently, the Doppler frequency shift, reckon the SAR antenna angle of view that is virtual to the orbital mechanical phenomenon rotation (Marghany 2009 b and Marghany 2011a). Consequently, the connection between the ocean surface dynamic orbital movement and also the SAR satellite orbital motion would be nonlinear attributable to the Doppler influence (Inglada and Garello 2002). In literature, there are many mathematical algorithms that are supported physical models to retrieve ocean surface current from SAR information. On alternative words, these algorithms area unit enforced to map the Doppler frequency spectra into the important ocean surface current speed. However, these techniques are restricted attributable to the nonlinear quality of ocean surface dynamic behaviours and radar signal (Marghany 2011a). In this regard, the Doppler rate has coarser resolution than radar cross section on the angle direction (Inglada and Garello 2002; Marghany 2009b and Marghany 2011b).

In this paper, we have a tendency to address the question of retrieving ocean surface current pattern from TanDEM-X data. This is often verified an exploitation of neural network technique. Hypotheses examined are: (i) Hopfield neural network based mostly multi-objective optimisation via Pareto dominance algorithmic rule is executed to TanDEM-X data; (ii) multi-objective optimisation via Pareto dominance is used as procedures for eliminating

inherent speckle from TanDEM-X data; and (iii); the nonlinearity of the physicist frequency shift is reduced multi-objective optimisation via Pareto dominance.

## 2. DATA ACQUISITION

### 2.1 Satellite Data

The TanDEM-X operational consequence involves the coordinated operation of 2 satellites flying in adjacent configuration. The alteration constraints for the formation are: (i) the orbits ascending nodes, (ii) the angle between the perigees, (iii) the orbit eccentricities and (iv) the phasing between the satellites. The observance of ocean currents is a vital facet of assessing climate changes. Space borne SAR along-track interferometry (ATI) has the promise to considerably contribute to the present field. It will offer large-area, world-wide surface current measurements. The matter of mapping relatively low velocities are often resolved by formations of SAR satellites that yield sufficiently sensitive ATI measurements (Romeiser and Runge 2007 and Romeiser et al., 2014).

In this study, the Hopfield algorithm relies on the TanDEM-X information. The TerraSAR-X and TanDEM-X satellites transmit identical SAR instruments working at 9.65 GHz frequency (X-band). Throughout some devoted operations, both satellites are placed associate exceedingly in a very special orbit configuration with a brief along track baseline providing a probability for current measurements. The data utilized in this study were nonheritable in StripMap (SM), bistatic (TS-X active / TD-X passive) mode and VV polarization.

### 2.2 In-situ Measurement

For the surface current knowledge acquisition, the Aquadopp® 2MHz current meter factory-made by Nortek AS (Figure1), Scandinavian country was used. The instrumentality could be a standalone instrumentation exploitation Doppler based mostly technology to measure surface currents at the deployment web site. The instrumentation is intended with intrinsically memory and internal battery pack wherever it may be designed to record and store information internally for self-deployment.



Figure 1. Aquadopp 2Mhz current meter deployment.

The Aquadopp® 2MHz current meter was deployed on coastal water of Teluk Kemang, Port Dickson, Malaysia on May 6 2017. (Figure 2). Two phases of data collection were carried out: (i) at 6:15 am to 8:15 am and (ii) at 6:15 pm to 8:15 pm. The surface current data was measured for intervals of 2 hours for both phases.

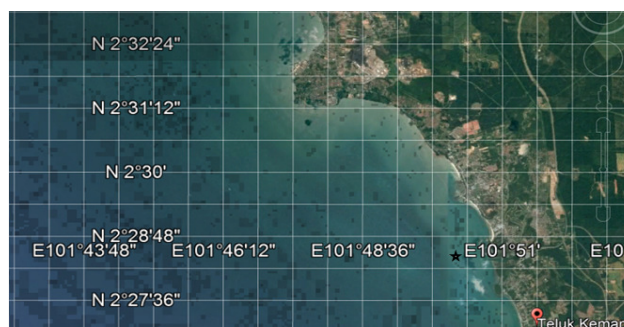


Figure 2. Geographical location of in situ measurements “☆”.

## 3 HOPFIELD ALGORITHM

Marghany (2015b) have implemented Hopfield neural networks for RADARSAT-2 SAR data to retrieve sea surface current. This section has been retrieved from Marghany (2015b) work. Therefore, Hopfield neural networks is used with TanDEM-X data. Consistent with Côté and Tatnall (1997), Hopfield neural networks is considered as a promising method for determining a minimum of energy of function. For instance, motion analysis and object pattern

recognitions might be coded into an energy function (Marghany 2004). Furthermore, the actual physical constraint, heuristics, or prior knowledge of sea surface features, nonlinearity and the Doppler frequency shift (Marghany 2009a) can be coded into the energy function.

A pattern, in the context of the  $N$  node Hopfield neural network is an  $N$ -dimensional vectors  $V = (v_1, v_2, \dots, v_n)$  and  $U = (u_1, u_2, \dots, u_n)$  from space  $S = \{-1, 1\}^N$ . A special subset of  $S$  is set of exemplar  $E = \{e^k : 1 \leq k \leq K\}$ , where  $e^k = (e^{k_1}, e^{k_2}, \dots, e^{k_n})$  and  $k$  is exemplar pattern where  $1 \leq k \leq K$ . The Hopfield net associates a vector from  $S$  with an exemplar pattern in  $E$ .

Following Marghany (2009b), Hopfield net is involved that  $w_{ij} = w_{ji}$  and  $w_{ii} = 0$ . Succeeding, Cao and Wang, (2003), the propagation rule  $\tau_i$  which defines how neuron sates and weight combined as input to a neuron can be described by

$$\tau_i = \sum_{j=1}^N f_i(j)w_{ij} \quad (1)$$

The Hopfield algorithm has consisted of (i) assign weights to synaptic connections; (ii) initialize the net with unknown pattern; and (iii) iterate until convergence and continue features tracking (Cote and Tatnall, 1997). First step of assign weight  $w_{ij}$  to synaptic connection can be achieved as understands:

$$w_{ij} = \begin{cases} \sum_{k=1}^K e_i^k e_j^k & \text{if } i \neq j \\ 0 & \text{if } i = j \end{cases} \quad (2)$$

Hopfield neural network could be identified current pattern features by mathematical comparing to each other in order to build an energy function (Liang and Wang, 2000 and Arik 2002). According to Côté and Tatnall (1997) the difference function to determine the discriminations between different features  $f_i, f_j$  by a given formula:

$$\begin{aligned} \text{diff}(f_i, f_j) = & G \cdot \max \left| \max \left( \frac{l_j}{l_i}, \frac{l_i}{l_j} \right) - L'', 0 \right| + H \cdot \max [\min |\theta_i - \theta_j|, 2\pi - |\theta_i - \theta_j| - \theta'', 0] \\ & + J \cdot \max [dis_{ij} - dist'', \theta''] \end{aligned} \quad (3)$$

where,  $L''$  is curvature shape of current feature,  $dis_{ij}$  is the distance between sea surface current features  $f_i$  and  $f_j$ , and  $G$  and  $H$  and  $J$  are constants, and  $\theta$  is an angle of orientation of local curve element. In addition,  $dist''$  and  $\theta''$  are the minimum acceptable distance and the maximum acceptable rotation angle, respectively before energy function.

#### 4. MULTI-OBJECTIVE OPTIMIZATION

Following Atashkari et al., (2004), the Multi-objective optimization (MOB) which is also termed the multi-criteria optimization or vector optimization. In this regard, it has been defined as finding a vector of decision variables satisfying constraints to give acceptable values to all objective functions. Generally, it can be mathematically defined

as: find the vector  $S^* = [S_1^*, S_2^*, \dots, S_n^*]^T$  to optimize

$$F(S) = [f_1(S), f_2(S), \dots, f_k(S)]^T, \quad (4)$$

subject to  $m$  inequality constraints

$$g_i(S) \leq 0, \quad i = 1 \text{ to } m, \quad (5)$$

and  $p$  equality constraints

$$h_j(S) = 0, \quad j = 1 \text{ to } p, \quad (6)$$

where  $S^* \in \mathfrak{R}^n$  is the vector of decision or design variables, and  $F(S) \in \mathfrak{R}^k$  is the vector of objective functions which each of them be either minimized or maximized. However, without loss of generality, it is assumed that all objective functions are to be minimized.

A point  $S^* \in \Omega$  ( $\Omega$  is a feasible region in  $\mathfrak{R}^n$  satisfying equations (4) and (6) is said to be Pareto optimal (minimal) with respect to the all  $S \in \Omega$  if and only if  $F(S^*) < F(S)$ . Alternatively, it can be readily restated as  $\forall i \in \{1, 2, \dots, k\}, \forall S \in \Omega - \{S^*\} f_i(S^*) \leq f_i(S) \wedge \exists j \in \{1, 2, \dots, k\} : f_j(S^*) < f_j(S)$ .

On other words, the solution  $S^*$  is said to be Pareto optimal (minimal) of ocean current pattern if no other solution can be found to dominate  $S^*$  using the definition of Pareto dominance. For a given MOP, the Pareto front  $PF^*$  is a set of vector of objective functions which are obtained using the vectors of decision variables in the Pareto set  $P^*$ , that is  $PF^* = \{F(S) = (f_1(S), f_2(S), \dots, f_k(S)) : S \in P^*\}$ . In other words, the Pareto front  $PF^*$  is a set of the vectors of objective functions mapped from  $P^*$  (Atashkari et al., 2004).

## 5. RESULTS AND DISCUSSION

The TanDEM-X data with X-band of the spotlight product which derived from the strip-map mode has utilized in this study. The Figure 3 indicates the results that are retrieved from Hopfield rule and Pareto rule. It is attention-grabbing realize that Pareto algorithmic rule has find the most effective solution for sea surface current pattern as compared to Hopfield neural network (Figure 3b). The morphology of ocean surface current structures are well known exploitation Pareto algorithmic rule. Indeed, random generation of 1000 iterations at intervals 3 min are needed to realize the performance of Pareto algorithmic program. Clearly, Pareto algorithm delivered spatial variation of surface current from onshore to offshore. Onshore surface current is dominated by maximum value of 0.12 m/s while the offshore surface currents have maximum value of 0.5 m/s.

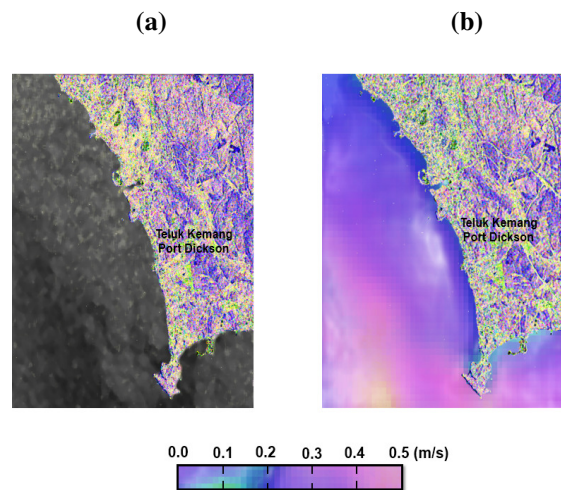


**Figure 3. Ocean current pattern simulated from (a) Hopfield neural network result (b) Pareto optimal solution.**

On the word of Mittermayer and Runge (2003), the velocity component of moving objects may be measured with ATI. The sensitivity of the instrument principally depends on the measuring device carrier frequency and consequently the effective time lag between the two measurements administered with two antennas and receiver chains. These parameters have to be compelled to be tailored to the speed range of the objects of interest. High speed objects like cars would like solely a really short time lag and also the two antennas acquired to be separated some meters.

Table 1 delivers the accuracy of this study. Clearly, the Pareto optimal solution has an excellent performance than Hopfield algorithm, with lowest P value of 0.00006 and RMSE of  $\pm 0.009$  and highest  $r^2$  of 0.86. Consistent with Marghany (2015b) and Marghany and Mansor (2016), the Hopfield neural network is anticipated as optimization tool to reduce the impact of the Doppler nonlinearity in the SAR data. Subsequently, multi-objective optimization is fairly deliberated as attaining a vector of verdict variables satisfying constraints to offer precise to all objective functions. This confirms study of Marghany and Mansor (2016).

**Table 1. Statistical regression of current meter sea surface current and retrieved one by Hopfield neural network based Pareto optimal solution.**

Methods	R <sup>2</sup>	RMSE (m/s)	P
Hopfield neural network- Current meter	0.78	±0.2	0.0006
Pareto optimal solution-Current meter	0.86	±0.009	0.000086

Moreover, the multi-objective optimisation via Pareto dominance obtains a particular curve that diminishes the inconsistency between the certain ocean surface current from TanDEMx data and in situ measurements. In this understanding, the new approach supported TanDEMx data and as a result the multi-objective optimisation via Pareto Dominance, know how to minimize the number of the residual faults for retrieving ocean surface current from TanDEMx data and delivers precise ocean surface current pattern spatial variation. This work recommends the work done by Atashkari et al., (2014) and Marghany (2015b). Additionally, it is recommended to utilize the time series of TanDEMx data for monitoring coastal current daily and seasonal variations.

## 6. CONCLUSIONS

This work geared toward retrieving ocean surface current from TanDEMx data along the coastal water of Port Dickson, Malaysia. Two approaches are prescribed: (i) Hopfield neural network rule; and (ii) Pareto optimum resolution. The study shows that the Pareto optimum resolution has highest performance than Hopfield neural network rule with lowest RMSE of ±0.009. Further, Pareto optimum resolution can verify the ocean surface current pattern variation on coastal water from TanDEMx data. Last, TanDEMx data reveals a superb guarantees for retrieving ocean surface current with X-band.

## References

- Alejandro, C. and Saadon, M.N., 1996, "Dynamic behaviour of the upper layers of the South China Sea", Proceedings of the National Conference on Climate Change, 12-13 August 1996, Universiti Pertanian Malaysia, Serdang. pp. 135-140.
- Alejandro, C., and Demmler, M.I., 1997, "Wind-driven circulation of Peninsular Malaysia's eastern continental shelf", *Sci. Mar.*, 61 (2), pp. 203-211.
- Arik S, (2002). A note on the global stability of dynamical neural networks," *Circuits and Systems I: Fundamental Theory and Applications, IEEE Transactions on*, vol. 49, pp. 502-504.
- Atashkari, K., Nariman-Zadeh, N., Darvizeh, A., Yao, X., Jamali, A., and Pilechi, A. 2004. Genetic design of GMDH-type neural networks for modelling of thermodynamically pareto optimized turbojet engines. *WSEAS Transactions on Computers*, 3(3), 719-724.
- Cote S and A. Tatnall, 1997. The Hopfield neural network as a tool for feature tracking and recognition from satellite sensor images, *International Journal of Remote Sensing*, vol. 18, pp. 871-885.
- Cao J. and J. Wang, 2003. Global asymptotic stability of a general class of recurrent neural networks with time-varying delays," *Circuits and Systems I: Fundamental Theory and Applications, IEEE Transactions on*, vol. 50, pp. 34-44.
- Inglada J. and R. Garello, 2002. On rewriting the imaging mechanism of underwater bottom topography by synthetic aperture radar as a Volterra series expansion, *Oceanic Engineering, IEEE Journal of*, vol. 27, pp. 665-674.
- Liang X.B. and J. Wang, 2000. Absolute exponential stability of neural networks with a general class of activation functions," *Circuits and Systems I: Fundamental Theory and Applications, IEEE Transactions on*, vol. 47, pp. 1258-1263.

Krieger, G., Fiedler, H., Mittermayer, J., Papathanassiou, K. and Moreira, A., 2003. Analysis of multistatic configurations for spaceborne SAR interferometry. *IEEE Proceedings-Radar, Sonar and Navigation*, 150(3), pp.87-96.

Marghany M. 2000. Finite Element Model of residual Currents and Oil spills Transport. Proceeding of IGARSS'2000. 24-28 July 2000. Honolulu, Hawaii. Vol. VI. pp:2513-2515.

Marghany M., 2003. Utilization of Hopfield Neural Network and Quasi-linear Model for Longshore Current Pattern Simulation from RADARSAT. CD-ROM Proceeding of IGARSS'2003, 20-25 July, Toulouse, France. pp:1-3.

Marghany M., 2004. Neural Network for Surface Current Trajectory Modelling from RADARSAT-1 SAR Data. Proceeding of 25<sup>th</sup> Asian Conference 22- 26 November 2004. Sheraton Chiang Mai Hotel, Chiang Mai, Thailand. Vol (1), pp: 362-366.

Marghany M. 2009a, "Robust model for retrieval sea surface current from different RADARSAT-1 SAR mode data," in *Signal and Image Processing Applications (ICSIPA), 2009 IEEE International Conference on*, 2009, pp. 492-495.

Marghany M 2009b. Volterra - Lax-wendroff algorithm for modelling sea surface flow pattern from jason-1 satellite altimeter data. Lecture Notes in Computer Science (including subseries Lecture Notes in Artificial Intelligence and Lecture Notes in Bioinformatics) Volume 5730 LNCS, 2009, Pages 1-18

Marghany M., 2011a. "Developing robust model for retrieving sea surface current from RADARSAT-1 SAR satellite data," *International Journal of Physical Sciences*, vol. 6, pp. 6630-6637.

Marghany M., 2011b. Three-dimensional coastal water front reconstruction from RADARSAT-1 synthetic aperture radar (SAR) satellite data. *International Journal of the Physical Sciences* Vol. 6(29), pp. 6653-6659.

Marghany, M. 2012. Three-Dimensional Coastal Front Visualization from RADARSAT-1 SAR Satellite Data. In Murgante B. et al. (eds.): *Lecture Notes in Computer Science (ICCSA 2012)*, Part III, LNCS 7335, pp. 447-456.

Maged Marghany 2013. Retrieving of Renewable Wave Energy from ENVISAT Satellite Data. Proceedings of the 34th Asian Conference on Remote Sensing 2013. Bali – Indonesia, October 20 -24, 2013. pp. SC03-657-SC03-663.

Marghany M., 2015a. Flock 1 data multi-objective evolutionary algorithm for turbulent flow detection. CD of 36th Asian Conference on Remote Sensing (ACRS 2015), Manila, Philippines, 24-28 October 2015. [a-a-r-s.org/acrs/administrator/components/com.../files/.../TH1-5-2.pdf](http://a-a-r-s.org/acrs/administrator/components/com.../files/.../TH1-5-2.pdf).

Marghany, M., 2015b, September. Simulation sea surface current from RADARSAT-2 SAR data using Hopfield neural network. In *Synthetic Aperture Radar (AP SAR), 2015 IEEE 5th Asia-Pacific Conference on* (pp. 805-808). IEEE.

Marghany M and Mansor S 2016. Retrieving Of Sea Surface Current Variations From Sentinel-1A Satellite Data. CD of 37th Asian Conference on Remote Sensing (ACRS), 37th ACRS from 17th - 21st October 2016, Galadari Hotel, Colombo, Sri Lanka, pp.1-6.

Mittermayer, J. and Runge, H., 2003, July. Conceptual studies for exploiting the TerraSAR-X dual receive antenna. In *INTERNATIONAL GEOSCIENCE AND REMOTE SENSING SYMPOSIUM* (Vol. 3, pp. III-2140).

Romeiser, R. and Runge, H., 2007. Theoretical evaluation of several possible along-track InSAR modes of TerraSAR-X for ocean current measurements. *IEEE Transactions on Geoscience and Remote Sensing*, 45(1), pp.21-35.

Romeiser, R., Suchandt, S., Runge, H., Steinbrecher, U. and Grunler, S., 2010. First analysis of TerraSAR-X along-track InSAR-derived current fields. *IEEE Transactions on Geoscience and Remote Sensing*, 48(2), pp.820-829.

Romeiser, R., Runge, H., Suchandt, S., Kahle, R., Rossi, C. and Bell, P.S., 2014. Quality assessment of surface current fields from TerraSAR-X and TanDEM-X along-track interferometry and Doppler centroid analysis. *IEEE Transactions on Geoscience and Remote Sensing*, 52(5), pp.2759-2772.